Supplement of

Viscosity and physical state of sucrose mixed with ammonium sulfate droplets

Rani Jeong et al.,

Correspondence to: Mijung Song (mijung.song@jbnu.ac.kr)

- SI_viscosity_Jeong_submitted.docx

S1. Measurements of bead speeds

Viscosity of a particle was determined by conversion from the bead speed inside a particle (Renbaum-Wolff et al., 2013a). The calibration curve was used for the conversion, which plotted and fitted the bead speeds measured at different RH values as a function of the known viscosity of sucrose/H_2O particles at the same RH (Fig. S1). In this study, we used $\textit{bead speeds} = 1.84\times10^{-4} \times (\textit{viscosity}, \eta)^{-1.08}$ equation from our previous study (Renbaum-Wolff et al., 2013a), which shows good agreement with the result for sucrose/H_2O particles in this study ($R^2 \approx 0.95$).

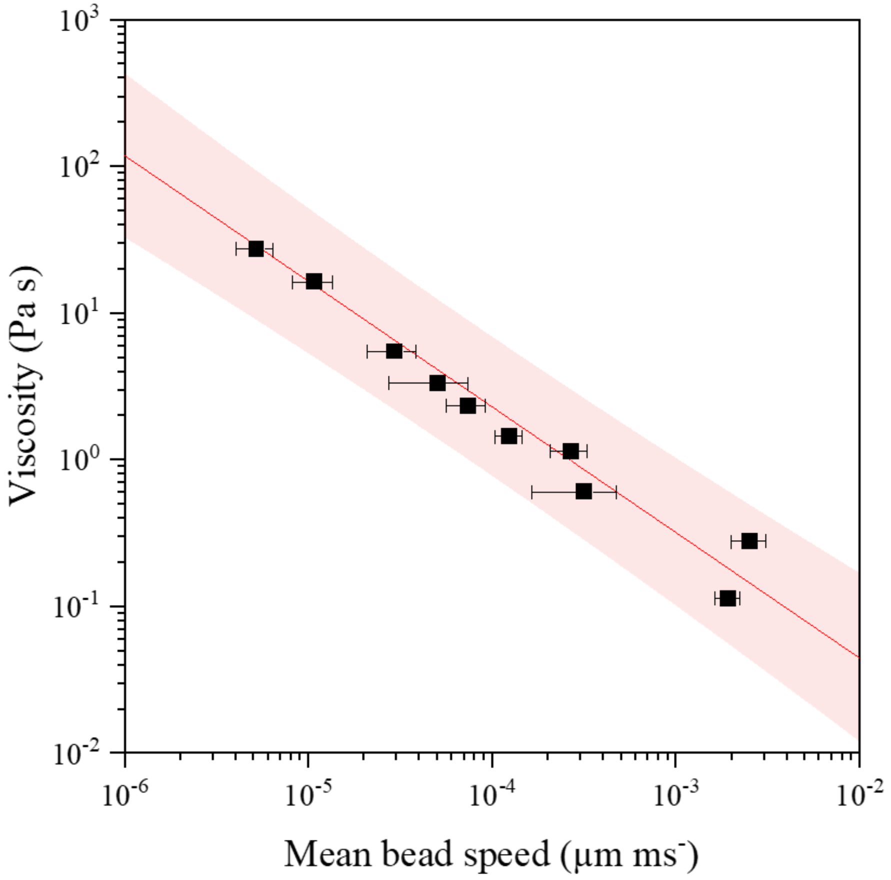

Figure S1: Calibration curve showing mean bead speeds as function of viscosities of sucrose/H_2O particles at different relative humidity (RH) values. The red curve is produced by a linear fit to the measurements, which yields the equation: $\textit{bead speeds} = 1.84\times10^{-4} \times (\textit{viscosity}, \eta)^{-1.08}$. The pink shaded envelope indicates 95% prediction bands of fitting to the data in this study. The error in mean bead speed (*x*-axis) is a standardization of 3-5 beads in one or two particles at given RH.

All bead speeds in Fig. S2 were converted to viscosity using the calibration curve in Fig. S1. Figure S2 (a) shows the mean bead speeds as a function of RH for sucrose/H_2O and AS/H_2O. The bead speeds of the sucrose/H_2O particles decreased from

~3 × 10^{-4} to ~2 × 10^{-5} µm · ms^{-1} when the RH decreased from ~83 % to ~69 %. The bead speeds of the AS/H_2O particles decreased from ~4 × 10^{-2} to ~1× 10^{-2} µm · ms^{-1} when the RH decreased from ~61 % to ~50 %. In Fig. S2 (b), the mean bead speeds measured at different RH values for sucrose/AS/H_2O particles with OIRs of 4:1, 1:1, and 1:4 are presented. The bead speeds of particles with OIR = 4:1 decreased from ~4 × 10^{-3} to ~9 × 10^{-6} µm · ms^{-1} when the RH decreased from ~80 % to ~52 %. The bead speeds of the particles with OIR = 1:1 decreased from ~1 × 10^{-2} to ~3 × 10^{-6} µm · ms^{-1} when the RH decreased from ~70 % to ~34 %; bead speeds of the particles with OIR = 1:4 decreased from ~2 × 10^{-2} to ~1 × 10^{-3} µm · ms^{-1} when the RH decreased from ~63 % to ~43 %.

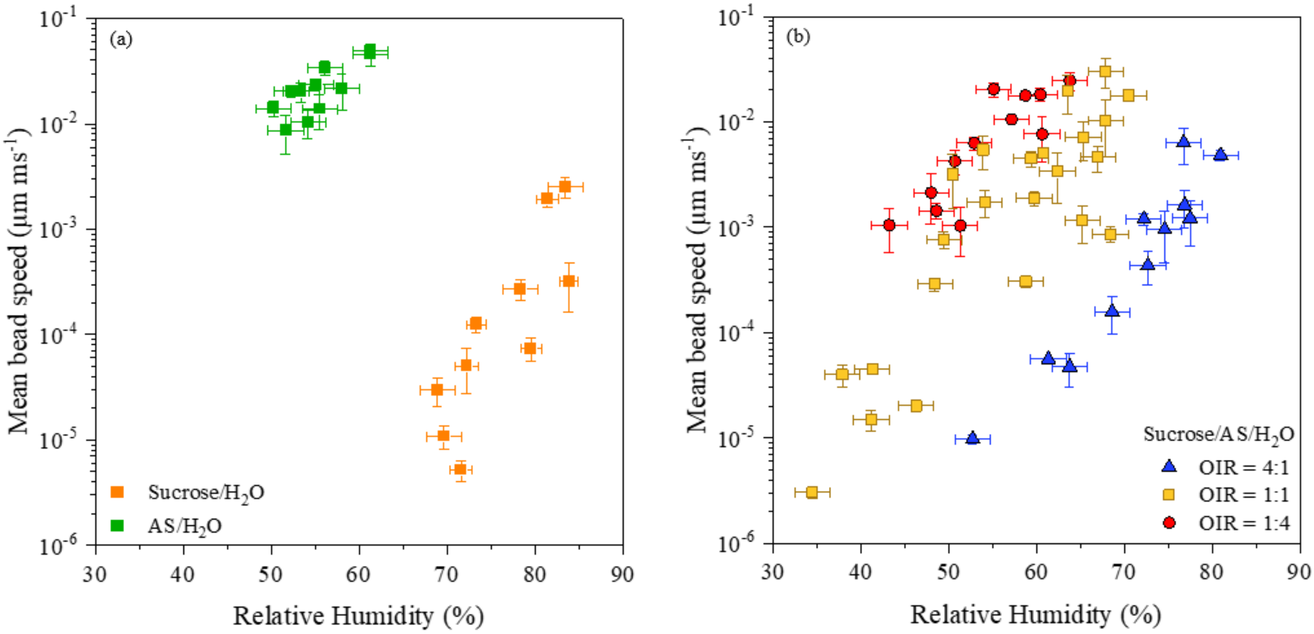

Figure S2: Mean bead speeds as a function of relative humidity (RH) for (a) binary systems of sucrose/H_2O and ammonium sulfate (AS)/H_2O, and (b) ternary systems of sucrose/AS/H_2O particles with organic-to-inorganic dry ratios (OIRs) = 4:1, 1:1, and 1:4. *X* error bars indicate uncertainties in the RH sensor calibration. *Y* error bars indicate standardization of 3-5 beads in one or two particles at given RH.

S2. Measurements of viscosity using poke-and-flow technique

Figure S3 shows the optical images of the sucrose/H_2O and sucrose/AS/H_2O particles for OIR = 4:1 during pre-poking, poking, post-poking. The experimental flow time was measured as the time taken for the area of the inner hole to decrease to 1/4 of the initial area based on the method of Renbaum-Wolff et al. (2013a) and Grayson et al. (2015). After the experimental flow time was measured, the lower limit of viscosity was calculated by the formula established in Sellier et al. (2015).

From the poke-and-flow experiment, the lower limit of viscosity was obtained by a fluid simulation (COMSOL) as described in previous studies (Renbaum-Wolff et al., 2013b; Grayson et al., 2015; Sellier et al., 2015); the particle geometry was fixed with a 20 μm quarter-sphere diameter which required the lower limit of physical parameters such as (i) density, (ii) contact angle, (iii) slip length and (iv) surface tension. Accordingly, the lower limit of (i) density was assumed to be equal to the density of pure water, (ii) contact angles were measured to be 87 ° ~ 93 ° for ~ 20 μl of all solutions on a hydrophobic substrate, and (iii) the lower limit of slip length was assumed to be 5 nm as described in previous studies (Churaev et al., 1984; Baudry et al., 2001; Joseph and Tabeling, 2005; Renbaum-Wolff et al., 2013b; Li et al., 2014; Grayson et al., 2015). In addition, (iv) the surface tension for sucrose and AS are available in the literature (Grayson et al., 2015; Dutcher et al., 2010). The lower limits of these physical parameters for all solutions, used in this study, fall within the range of the lower limits used in previous studies that used the same technique, i.e., poke-and-flow (Renbaum-Wolff et al., 2013b; Grayson et al., 2015; Song et al., 2016a, 2019; Song et a., 2021). Therefore, the lower limit of the viscosity was defined as ~10^8 Pa·s when a particle cracked during poke-and-flow experiments.

(a) Sucrose/H_2O

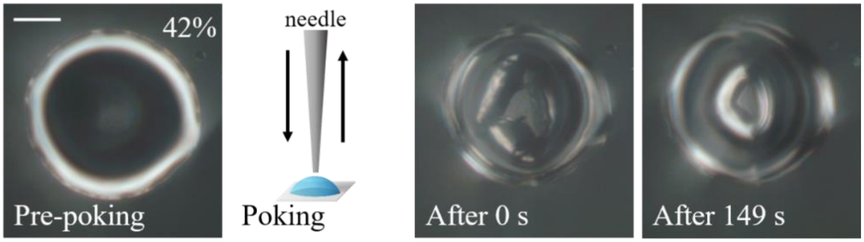

(b) Sucrose/AS/H_2O for OIR = 4:1

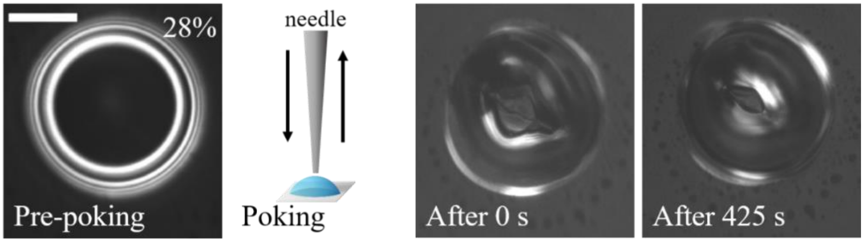

Figure S3: Optical images for experimental flow times ($\tau_{(exp,\ flow)}$) during poke-and-flow experiments at 293 ± 1 K on pre-poking, poking, and post-poking for particles consisting of (a) sucrose/H_2O and (b) sucrose/ammonium sulfate (AS)/H_2O for organic-to-inorganic dry ratio (OIR) = 4:1. White scale bar indicates 20 µm.

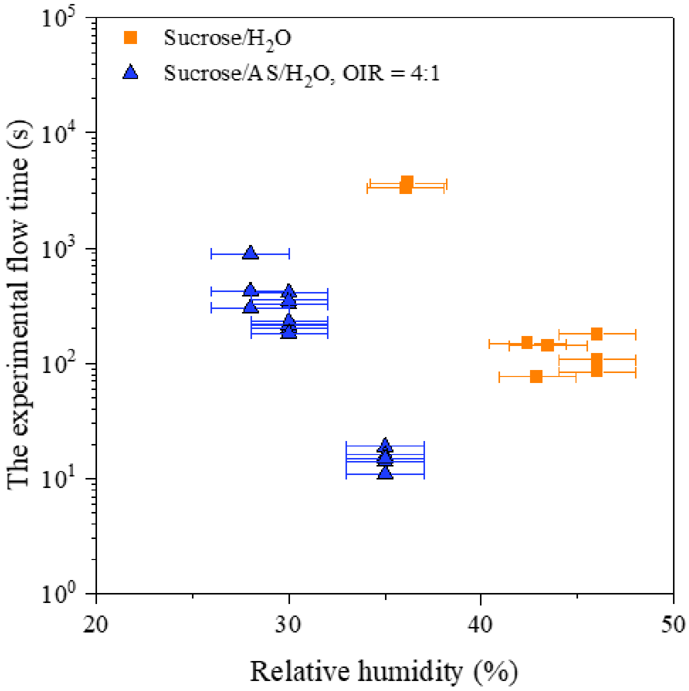

Figure S4: Experimental flow time of sucrose/H_2O and sucrose/ammonium sulfate (AS)/H_2O particles for organic-to-inorganic dry ratio (OIR) = 4:1 as a function of relative humidity (RH) from poke-and-flow experiments at 293 ± 1 K. The *x* error bars indicate the uncertainty in the RH calibration. The viscosity of sucrose/H_2O and sucrose/AS/H_2O particles with OIR = 4:1 (Fig. 4) indicate standardization of 2-8 particles as a result of poke-and-flow experiments at given RH.

S3. Comparison of additional AIOMFAC-VISC model settings

Figure S5 shows how the measurements align with the default aquelec mixing approach in AIOMFAC-VISC compared to the ZSR mixing approach shown in Fig. 4 of the main text.

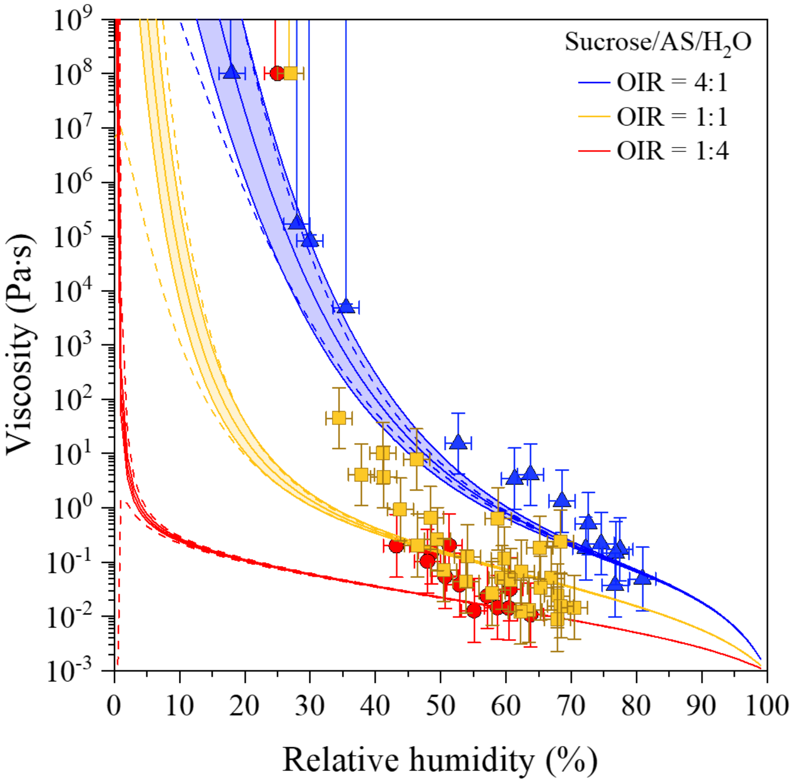

Figure S5: Comparison of viscosity measurements from bead-mobility and poke-and-flow experiments (squares) and Aerosol Inorganic–Organic Mixtures Functional groups Activity Coefficients Viscosity model (AIOMFAC-VISC) predictions (solid curves) of ternary mixtures of sucrose/ammonium sulfate (AS)/H_2O at varying organic-to-inorganic dry ratios (OIRs) at 293 ± 1 K. AIOMFAC-VISC predictions with the aquelec mixing model. Model sensitivity, defined by the impact of ± 2% variation in aerosol water content, is shown by the dashed curves. Shaded regions show the potential viscosity prediction error introduced by ± 5% error in the glass transition temperature of sucrose. See also Fig. 4.

References

Baudry, J., Charlaix, E., Tonck, A., and Mazuyer, D.: Experimental evidence for a large slip effect at a nonwetting fluid-solid interface, Langmuir, 17, 5232–5236, doi:10.1021/La0009994, 2001.

Churaev, N. V., Sobolev, V. D., and Somov, A. N.: Slippage of liquids over lyophobic solid-surfaces, J. Colloid Interf. Sci., 97, 574–581, doi:10.1016/0021-9797(84)90330-8, 1984.

Dutcher, C. S., Wexler, A. S. and Clegg, S. L.: Surface tensions of inorganic multicomponent aqueous electrolyte solutions and melts, J. Phys. Chem. A, 114(46), 12216–12230, doi:10.1021/jp105191z, 2010.

Grayson, J., Song, M., Sellier, M., and Bertram, A.: Validation of the poke-flow technique combined with simulations of fluid flow for determining viscosities in samples with small volumes and high viscosities, Atmos. Meas. Tech., 8, 2463-2472, https://doi.org/10.5194/amt-8-2463-2015, 2015.

Joseph, P. and Tabeling, P.: Direct measurement of the apparent slip length, Phys. Rev. E., 71, 035303, doi:10.1103/Physreve.71.035303, 2005.

Koop, T., Bookhold, J., Shiraiwa, M., and Pöschl, U.: Glass transition and phase state of organic compounds: dependency on molecular properties and implications for secondary organic aerosols in the atmosphere, phys. Chem. Chem. Phys., 13, 19238-19255, https://doi.org/10.1039/C1CP22617G, 2011.

Li, L., Mo, J. W., and Li, Z. L.: Flow and slip transition in nanochannels, Phys. Rev. E., 90, 033003, doi:10.1103/Physreve.90.033003, 2014.

Renbaum-Wolff, L., Grayson, J., and Bertram, A.: New methodology for measuring viscosities in small volumes characteristic of environmental chamber particle samples, Atmos. Chem. Phys., 13, 791-802, https://doi.org/10.5194/acp-13-791-2013, 2013a.

Renbaum-Wolff, L., Grayson, J. W., Bateman, A. P., Kuwata, M., Sellier, M., Murray, B. J., Shilling, J. E., Martin, S. T., and Bertram, A. K.: Viscosity of α-pinene secondary organic material and implications for particle growth and reactivity, Proc. Natl. Acad. Sci. U. S. A., 110, 8014-8019, https://doi.org/10.1073/pnas.1219548110, 2013b.

Sellier, M., Grayson, J. W., Renbaum-Wolff, L., Song, M. and Bertram, A. K.: Estimating the viscosity of a highly viscous liquid droplet through the relaxation time of a dry spot, J. Rheol., 59(3), 733–750, doi:10.1122/1.4917240, 2015.

Song, M., Liu, P. F., Hanna, S. J., Zaveri, R. A., Potter, K., You, Y., Martin, S. T., and Bertram, A. K.: Relative humidity-dependent viscosity of secondary organic material from toluene photo-oxidation and possible implications for organic particulate matter over megacities, Atmos. Chem. Phys., 16, 8817-8830, https://doi.org/10.5194/acp-16-8817-2016, 2016a

Song, M., Maclean, A. M., Huang, Y., Smith, N. R., Blair, S. L., Laskin, J., Laskin, A., DeRieux, W.-S. W., Li, Y., and Shiraiwa, M.: Liquid–liquid phase separation and viscosity within secondary organic aerosol generated from diesel fuel vapors, Atmos. Chem. Phys., 19, 12515-12529, https://doi.org/10.5194/acp-19-12515-2019, 2019.

Song, Y., Lilek, J., Lee, J. B., Chan, M. N., Wu, Z., Zuend, A., and Song, M.: Viscosity and phase state of aerosol particles consisting of sucrose mixed with inorganic salts, Atmos. Chem. Phys., 1-32, https://doi.org/10.5194/acp-2021-110, 2021.